



7-20-2017

Inverse Kinematics Proton Scattering of P41

Benjamin R. Klybor

Ursinus College, beklybor@ursinus.edu

Follow this and additional works at: https://digitalcommons.ursinus.edu/physics_astro_sum



Part of the [Nuclear Commons](#)

Click here to let us know how access to this document benefits you.

Recommended Citation

Klybor, Benjamin R., "Inverse Kinematics Proton Scattering of P41" (2017). *Physics and Astronomy Summer Fellows*. 14.
https://digitalcommons.ursinus.edu/physics_astro_sum/14

This Paper is brought to you for free and open access by the Student Research at Digital Commons @ Ursinus College. It has been accepted for inclusion in Physics and Astronomy Summer Fellows by an authorized administrator of Digital Commons @ Ursinus College. For more information, please contact aprock@ursinus.edu.

Inverse Kinematics Proton Scattering of ^{41}P

B. R. Klybor

Ursinus College, Michigan State University

(Dated: July 20, 2017)

Abstract

We have measured the γ -ray spectrum of ^{41}P using proton scattering in inverse kinematics with the NSCL/Ursinus College liquid hydrogen target and the GRETINA γ -ray tracking array. We present preliminary results, including γ -ray intensities and branching ratios.

INTRODUCTION

Endeavors to expand knowledge about exotic nuclei require ever more powerful accelerator facilities and γ -ray detection arrays in order to study exotic nuclei. Of greatest interest are those exotic nuclei in the neighborhood of magically numbered nuclei such as ^{48}Ca . By measuring γ -ray spectra, constructing level schemes, and measuring excitation cross sections we can gain greater understanding of nuclear structure. In this experiment we used the Coupled Cyclotron Facility at the National Superconducting Cyclotron Laboratory and the GRETINA γ -ray tracking array [1] to measure γ -rays emitted by exciting ^{41}P nuclei by inverse kinematics proton scattering on a liquid hydrogen target. A prior γ -ray spectroscopy measurement of ^{41}P [2] has given us a good starting point on which to base our analysis. Here we present preliminary results and analysis.

EXPERIMENT

The experiment began with a primary beam consisting of ^{48}Ca accelerated by the K500-K1200 coupled cyclotrons at 140 MeV/u. The beam was then fragmented on a 1222 mg/cm² ^9Be production target and then further separated by Z using a 300 mg/cm² Al wedge at the intermediate image of the A1900 fragmentation separator [3]. After passing through the A1900, the beam consisted primarily of ^{41}P (84%), our nucleus of interest, and smaller, though non-negligible, amounts of ^{39}Si (3%) and ^{42}S (12%). Prior to moving into the S800 magnetic spectrograph [4] the beam passed through the NSCL/Ursinus College liquid hydrogen target.

The liquid hydrogen was maintained at 17 K and 880 Torr and had a density of 74.44 kg/m². The target was constructed of a 30 mm thick aluminum cylinder with two 125 μm Kapton entrance and exit windows. Surrounding the target was a 1 mm thick aluminum radiation shield with entrance/exit windows which were then covered in a layer of 5 μm aluminized Mylar foil. As the beam passed through the target the GRETINA γ -ray tracking array [1] recorded gamma rays. GRETINA consisted of 32 36-fold segmented high purity Ge crystals placed in eight clusters of four crystals each in a hemisphere around the target in order to accommodate the liquid hydrogen cooling system.

After passing through the liquid hydrogen target, the scattered beam particles moved

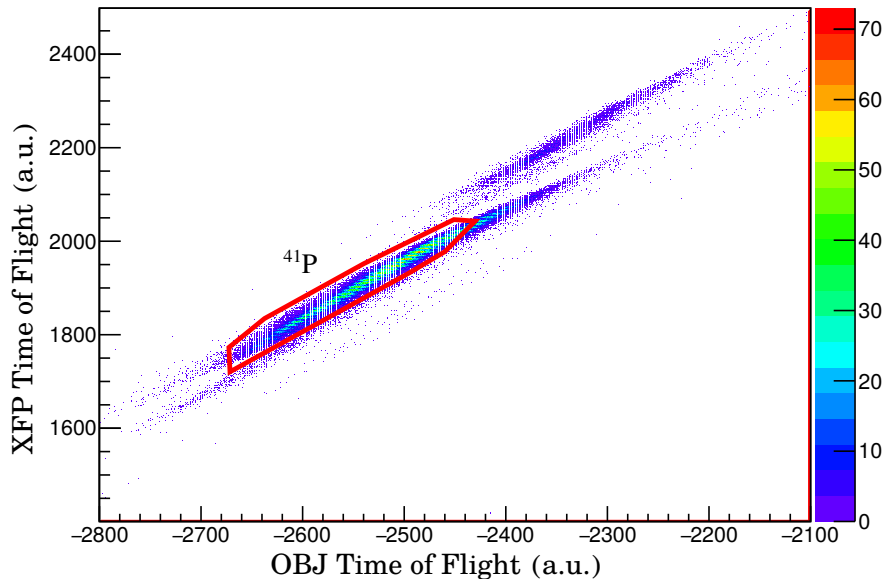


FIG. 1. The incoming particle identification spectrum generated by the time stamp from the S800 object box scintillator (OBJ) on the horizontal axis and that from the A1900 extended focal plane scintillator (XFP) on the vertical axis. The E1 scintillator in the S800 focal plane triggers start of timing. The red contoured region is the cut for ^{41}P .

into the S800 magnetic spectrograph which was used for particle identification (PID) and to measure the kinetic energies and trajectories of scattered particles. We collected all GRETINA-S800 coincidences as well as downscaled (by 100) S800 events. We collected the latter in order to determine the total particles passing through the target during the experiment. PID consisted of incoming and outgoing ^{41}P gates. Fig. 1 shows the PID spectrum of incoming particles, comparing the time of flight measurement from the object box (OBJ), located upstream of the target at the beginning of the S800, to the E1 scintillator, located in the focal plane of the S800, with that from the extended focal plane scintillator (XFP) located upstream of the target in the A1900 to the E1 scintillator in arbitrary units. By comparing these times of flight we can positively identify incoming nuclei by charge to mass ratio since particles with larger charge to mass ratios will have longer times of flight measurements. Fig 2 shows the gated outgoing PID spectrum by comparing the time of flight measurement from the OBJ scintillator to the E1 scintillator with the energy loss recorded by the ion chamber at the end of the S800. We isolated the proton-scattering

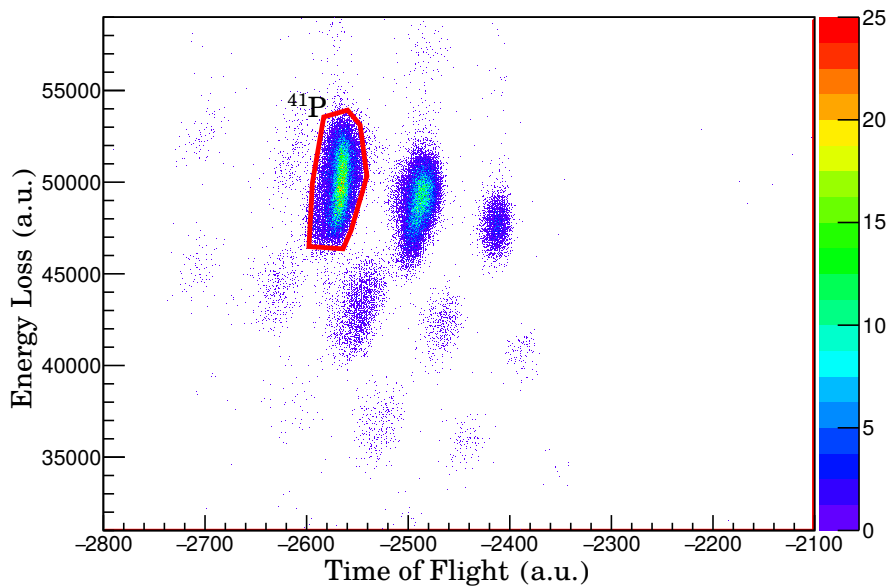


FIG. 2. The energy loss of triggered events compared to time of flight from the S800 OBJ scintillator to the E1 scintillator in the focal plane of the S800. The red contour is the cut for ^{41}P .

reactions by applying ^{41}P cuts to both the incoming and the outgoing PID spectra.

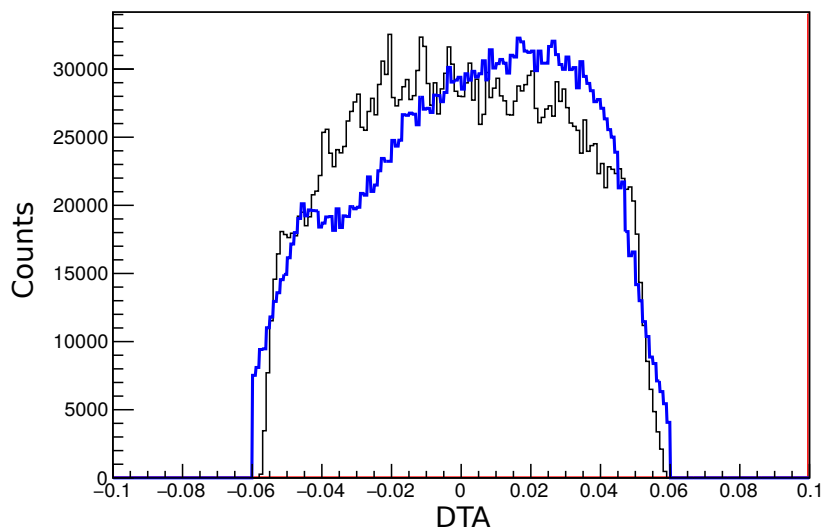


FIG. 3. The incoming relative kinetic energy spectrum for ^{41}P . Simulated spectrum (blue) is overlaid the measured spectrum (black). Simulated target bulge thickness is 0.92 mm.

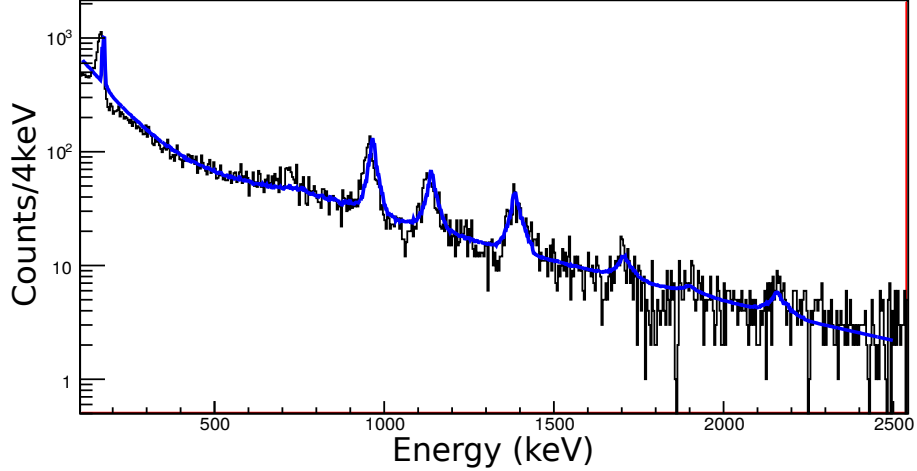


FIG. 4. An initial γ -ray spectrum fit (blue) to the experimental γ -ray spectrum (black) for ^{41}P . An average incoming beam velocity of $\beta = v/c = 0.3364$ was used to Doppler correct GREYINA-S800 coincidence events.

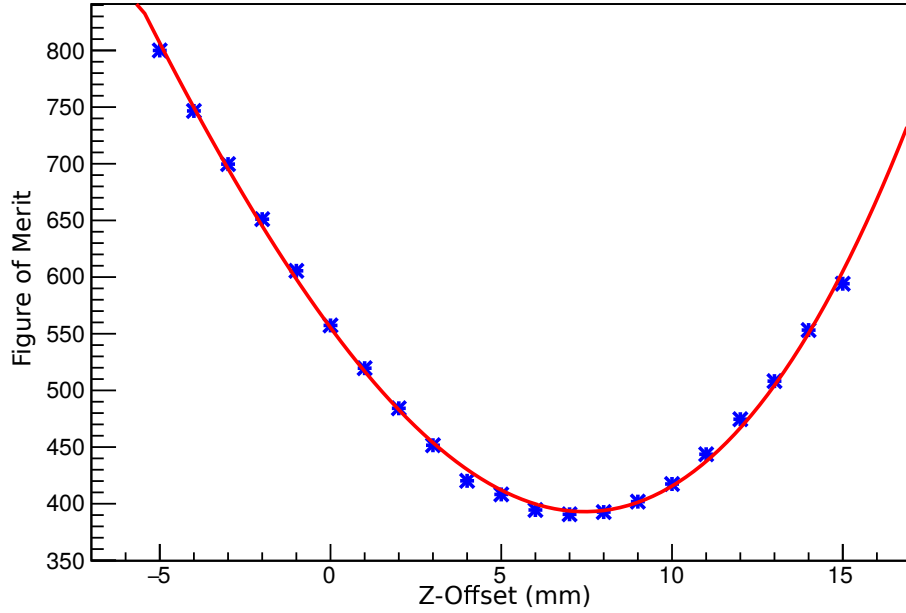


FIG. 5. The figure of merit from log-likelihood fits to outgoing kinetic energy distributions by target z-offset.

ANALYSIS

We used the average velocity, which we obtained from the simulation of the beam traversing the target described above, for Doppler reconstruction of the γ -ray spectrum. Fig. 4 shows the Doppler-corrected experimental (black) and simulated (blue) γ -ray spectrum. We

observed the γ rays at 172, 964, 1146, and 1408 keV reported by Bastin et al. [2]. The 420 keV γ -ray observed by Bastin et al. [2] was not observed. We also observed two new photopeaks whose initial values we determined to be 730 and 1709 keV.

In order to fit simulations to the measured γ -ray spectrum, we first needed to determine the bulge thickness of the Kapton windows - due to the pressure required to maintain liquid hydrogen - since the thickness of these windows significantly affects the target thickness and thereby Doppler reconstruction and cross sections. The goal of gating and sorting data to determine this bulge thickness resulted in Fig. 3, an outgoing kinetic energy distribution of incoming nuclei of experimental data (black) and simulated data (blue). By using the GEANT4 physical simulator [5] to fit simulated outgoing kinetic energy distributions with different bulge thicknesses we were able to interpolate the average bulge thickness through which ^{41}P nuclei involved in proton scattering passed by minimizing the figure of merit associated with each log-likelihood fit. This GEANT4 also determined the target thickness used to calculate cross sections.

In addition, we used simulations to optimize the position of the target, along the beam axis. The z-offset is a significant factor in Doppler reconstruction, because it determines the average position from which γ rays are emitted. In order to optimize the z-offset we used GEANT4 and ROOT to fit simulated γ -ray spectra to the experimental γ -ray spectrum, minimizing the figure of merit by varying the z-offset value and interpolating the z-offset value which gives the lowest figure of merit as shown in Fig. 5. For these fits we used the literature values for the photopeaks observed by Bastin et al [2], and the Gaussian centroid for new photopeaks. Finally using the optimal bulge thickness and z-offset values we then used the average velocity of the simulated beam passing through the target to Doppler reconstruct the γ -ray spectrum of ^{41}P .

To determine the Doppler corrected γ -ray energy for each photopeak, we varied the energy of simulated γ rays, minimizing the figure of merit to find the optimal values. The fully Doppler corrected γ -ray spectrum with these energies is given in Fig. 7. The 172, 967, 1142, and 1404 keV γ rays we report are well within the error ranges of those reported by Bastin et al [2], though even with optimization we did not observe the 420 keV γ ray. We also measured a lifetime for the 172 keV state of 385 ps by varying the lifetime of simulated 172 keV photopeaks, minimizing the figure of merit from these fits. In addition we observed two new γ rays at 727 and 1723 keV. While the 727 keV γ ray is in coincidence with the 1404-172

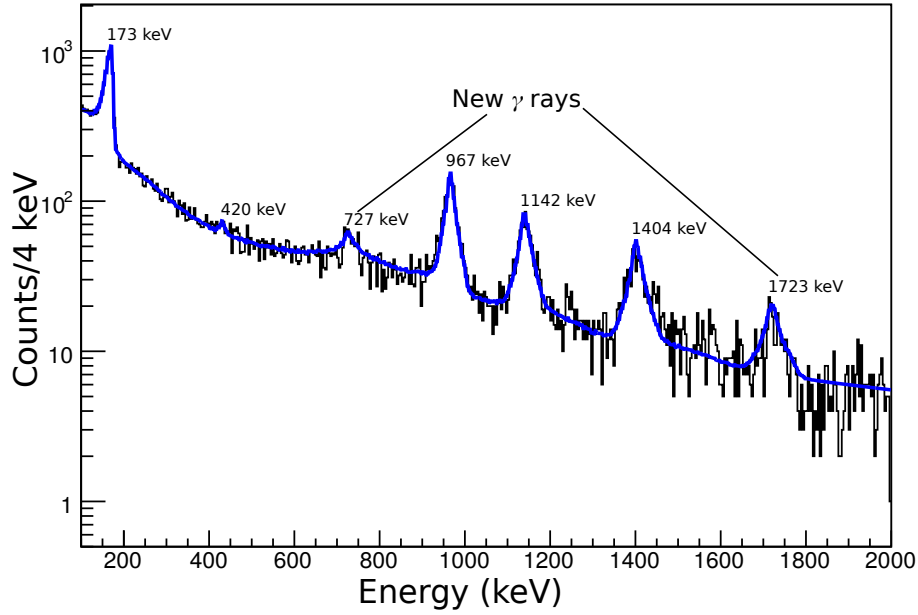


FIG. 6. The optimized, Doppler corrected γ -ray spectrum for ^{41}P . An incoming beam velocity of $\beta = v/c = 0.3364$ was used for Doppler reconstruction.

keV cascade, the 1723 is not in coincidence with any other γ rays, so we were unable to place it in the level scheme. Fig. 7 shows the complete level scheme where the thickness of the transition lines show relative intensity proportional to the most intense γ ray observed, 172 keV.

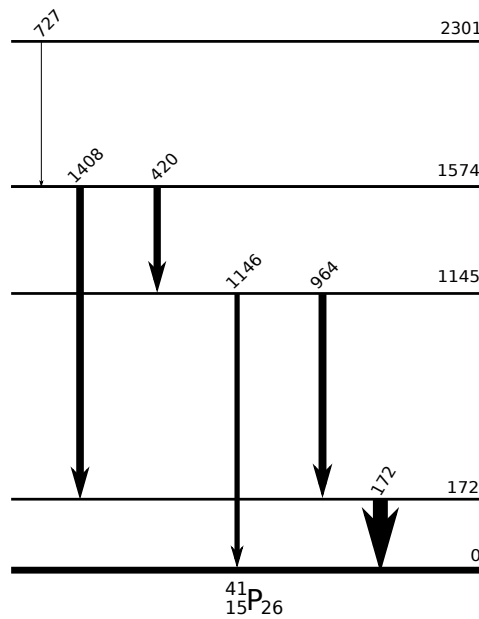


FIG. 7. Our proposed energy level diagram for ^{41}P .

TABLE I. The γ -ray energies, γ -ray intensities, and branching ratios of ^{41}P excitations. We show literature values from Bastin et al [2] for comparison.

	Literature Values			Present work		
	E_{level} [keV]	E_{γ} [keV]	BR [%]	E_{γ} [keV]	I_{γ} [%]	BR [%]
^{41}P	172	172(12)		172(0.1)	100(2)	
	1145	964(22)	80.0(14)	967(0.9)	58(4)	62(4)
		1146(28)	20.0(16)	1142(1)	35(6)	38(7)
	1547	420(22)		431(10)	< 49	6(3)
		1408(19)	86(5)	1404(2)	> 51	94(6)
	2301			727(3)	4(31)	
			1723(4)	14(12)		

This work was supported by the National Science Foundation under Grant No. PHY-1617250. GRETINA was funded by the US DOE - Office of Science. Operation of the array at NSCL is supported by NSF under Cooperative Agreement No. PHY-1102511(NSCL) and DOE under Grant No. DE-AC02-05CH11231 (LBNL). We also thank T. J. Carroll for the use of the Ursinus College Parallel Computing Cluster, which is supported by NSF Grant No. PHY-1607335.

-
- [1] I.-Y. Lee, Journal of Physics: Conference Series **420**, 012156 (2013).
- [2] B. Bastin, S. Grévy, D. Sohler, O. Sorlin, Z. Dombrádi, N. L. Achouri, J. C. Angélique, F. Azaiez, D. Baiborodin, R. Borcea, C. Bourgeois, A. Buta, A. Bürger, R. Chapman, J. C. Dalouzy, Z. Dlouhy, A. Drouard, Z. Elekes, S. Franchoo, S. Iacob, B. Laurent, M. Lazar, X. Liang, E. Liénard, J. Mrazek, L. Nalpas, F. Negoita, N. A. Orr, Y. Penionzhkevich, Z. Podolyák, F. Pougheon, P. Roussel-Chomaz, M. G. Saint-Laurent, M. Stanoiu, I. Stefan, F. Nowacki, and A. Poves, Physical Review Letters **99**, 022503 (2007).
- [3] D. J. Morrissey, B. M. Sherrill, M. Steiner, A. Stolz, and I. Wiedenhoever, Nuclear Instruments and Methods in Physics Research Section B: Beam Interactions with Materials and Atoms **204**,

90 (2003).

- [4] D. Bazin, J. A. Caggiano, B. M. Sherrill, J. Yurkon, and A. Zeller, Nuclear Instruments and Methods in Physics Research Section B: Beam Interactions with Materials and Atoms **204**, 629 (2003).
- [5] S. Agostinelli, J. Allison, K. Amako, J. Apostolakis, H. Araujo, P. Arce, M. Asai, D. Axen, S. Banerjee, G. Barrand, F. Behner, L. Bellagamba, J. Boudreau, L. Broglia, A. Brunengo, H. Burkhardt, S. Chauvie, J. Chuma, R. Chytrcek, G. Cooperman, G. Cosmo, P. Degt-yarenko, A. Dell’Acqua, G. Depaola, D. Dietrich, R. Enami, A. Feliciello, C. Ferguson, H. Fesefeldt, G. Folger, F. Foppiano, A. Forti, S. Garelli, S. Giani, R. Giannitrapani, D. Gibin, J. J. Gmez Cadenas, I. Gonzalez, G. Gracia Abril, G. Greeniaus, W. Greiner, V. Grichine, A. Grossheim, S. Guatelli, P. Gumplinger, R. Hamatsu, K. Hashimoto, H. Hasui, A. Heikkinen, A. Howard, V. Ivanchenko, A. Johnson, F. W. Jones, J. Kallenbach, N. Kanaya, M. Kawabata, Y. Kawabata, M. Kawaguti, S. Kelner, P. Kent, A. Kimura, T. Kodama, R. Kokoulin, M. Kossov, H. Kurashige, E. Lamanna, T. Lampn, V. Lara, V. Lefebure, F. Lei, M. Liendl, W. Lockman, F. Longo, S. Magni, M. Maire, E. Medernach, K. Minamimoto, P. Mora de Freitas, Y. Morita, K. Murakami, M. Nagamatu, R. Nartallo, P. Nieminen, T. Nishimura, K. Ohtsubo, M. Okamura, S. O’Neale, Y. Oohata, K. Paech, J. Perl, A. Pfeiffer, M. G. Pia, F. Ranjard, A. Rybin, S. Sadilov, E. Di Salvo, G. Santin, T. Sasaki, N. Savvas, Y. Sawada, S. Scherer, S. Sei, V. Sirotenko, D. Smith, N. Starkov, H. Stoecker, J. Sulkimo, M. Takahata, S. Tanaka, E. Tcherniaev, E. Safai Tehrani, M. Tropeano, P. Truscott, H. Uno, L. Urban, P. Urban, M. Verderi, A. Walkden, W. Wander, H. Weber, J. P. Wellisch, T. Wenaus, D. C. Williams, D. Wright, T. Yamada, H. Yoshida, and D. Zschesche, Nuclear Instruments and Methods in Physics Research Section A: Accelerators, Spectrometers, Detectors and Associated Equipment **506**, 250 (2003).